Optimization of Highly Efficient Monolayer $MoSe_2$ Based Solar Cells

B. Zaidi[a,*], C. Shekhar[b], B. Hadjoudja[c], S. Gagui[c] and B. Chouial[c]
[a]Department of Physics, Faculty of Material Sciences, University of Batna 1, Batna, Algeria
[b]Department of Applied Physics, Amity University Gurgaon, Haryana, India 122413
[c]Laboratory of Semiconductors, Department of Physics, University of Badji-Mokhtar, Annaba, Algeria

(Received March 21, 2019; revised version June 13, 2019; in final form June 25, 2019)

The effect of $MoSe_2$ thin films on the solar photovoltaic characteristics of ZnO/ZnS/$MoSe_2$ has been studied. The variation in the efficiency of the solar cells as a funcion of the thickness of the $MoSe_2$ layer, characteristic (J–V), and the quantum efficiency (QE) of the solar cell for different energies of the incident radiation have been studied. The results indicate that when the thickness of $MoSe_2$ is increased the efficiency of $MoSe_2$ based solar cells improves from 9.24% to 17.51%. The output photovoltaic parameters such as the efficiency is found to be 17.51% and a good short circuit current J_{sc} value of 22.19 mA/cm^2 is attained and the corresponding open circuit voltage V_{oc} is 0.8 V.

DOI: 10.12693/APhysPolA.136.495
PACS/topics: ZnO, ZnS, $MoSe_2$, Solar cells, SCAPS-1D.

1. Introduction

As the demand for the inexpensive electric power is increasing, the demand for the innovative approach for the solar cell design using novel materials that can show comparable photovoltaic conversion with the current technologies based on crystalline silicon or CIGS films [1–5] is also increasing. $MoSe_2$ shows high electrical conductivity ($\sigma = 1 \times 10^{-3}$ s m^{-1}) and hence, is metallic in nature [6]. $MoSe_2$ based solar cells have superior performance in photo-electo-chemical systems compared to the other dichalcogenides [7]. In the bulk form $MoSe_2$ has indirect band gap and can have the direct band gap in case of a thin film. This property of the $MoSe_2$ have been used to employ thin film $MoSe_2$ in many applications including LEDs, light harvesting, optical sensors etc. [8]. The solar cells based on SnS and CZTS absorber materials can yield the desired performance in the long term. numerical studies have been developed using analysis of photonic and microelectronic structures (SCAPS-1D) to reveal efficiencies of cells under standard AM1.5 illumination conditions based on heterojunction [9–13]. The transition metal dichalcogenides such as $MoSe_2$, MoS_2, WSe_2, and WS_2 are extensively studied due to their resemblance to graphene properties [14–17]. Bulk Mo(S,Se)$_2$ are indirect semiconductors, whereas their monolayers exhibit a direct gap, making them attractive for optoelectronics [18]. the mose$_2$ monolayer has an ultra-thin lamellar structure with thickness about 0.65 nm [19], a direct band gap of 1.6 eV [20], and high electron mobility of 100 cm^2 V^{-1} s^{-1} [21]. In this work, we optimize the photovoltaic parameters of $MoSe_2$ based solar cells by using SCAPS-1D. The present device architecture is envisaged as a potentially valuable candidate for high performance photovoltaic device.

*corresponding author; e-mail: zbeddiaf@gmail.com

2. Material parameters

In Fig. 1 the schematic diagram of the proposed device is shown. With the schematic diagram, the front contacts (exposed to light) on the left side, and the rear contacts on the right are also displayed by SCAPS-1D convention. The Shockley-Read-Hall (SRH) interface approach allows carriers from both conduction and valence bands to participate in the interface recombination process. The solar cell structure consists of three different layers: ZnO (antireflective), ZnS (buffer), and $MoSe_2$ monolayer (absorber).

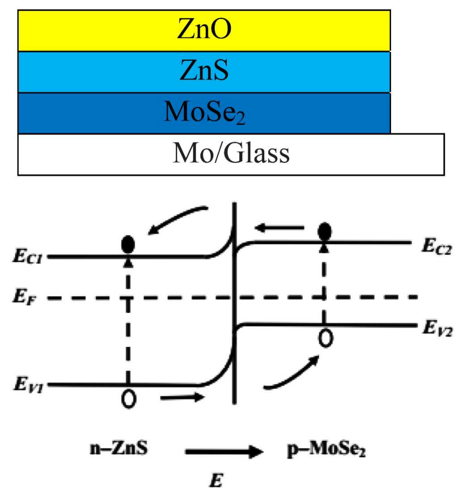

Fig. 1. Structure and the energy band diagram of the solar cell simulated by using SCAPS-1D.

Figure 1 describes the different layers of the materials used in the part of a PV device and the conventions used in this study under the following parameters: solar spectrum AM1.5, P = 100 mW/cm^2, and T = 300 K. Details of Materials parameters used in SCAPS-1D simulation are given in Table I.

TABLE I

Materials Parameters used in SCAPS-1D simulation.

Parameters	n-ZnO	n-ZnS	p-$MoSe_2$
Thickness [μm]	0.080	0.100	0.1 to 0.4
E_g [eV]	3.4	3.5	1.6
μ_n [cm/V s]	100	100	100
μ_p [cm/V s]	25	25	25
N_a [cm^{-3}]	10^{14}	10^{14}	10^{14}
N_d [cm^{-3}]	10^{20}	10^{20}	10^{6}

3. Results and discussion

The effect of variation in thickness of $MoSe_2$ on efficiency is shown in Fig. 2. It is found that the increase in thickness of $MoSe_2$ leads to increase in efficiency. We can note that the efficiency of solar cell increases from 9.3% to 17.5% as the thickness of $MoSe_2$ is increased from 0.1 to 0.4 μm. Therefore, we can obtain the best efficiency of the solar cell up to 17.5% for the thickness of $MoSe_2$ at 0.4 μm.

Figure 3 shows the simulated ($J - V$) characteristic of $MoSe_2$ based solar cells under AM1.5 illumination (100 mW/cm^2) and T = 300 K. In this stage the optimum thickness of $MoSe_2$ layer was set to 0.4 μm. The (J–V) curve reveals that the model predicts short-circuit current densities J_{sc} (22.19 mA/cm^2) and open-circuit voltages V_{oc} (0.8 V). We can see that V_{oc} and J_{sc} are much larger than the results achieved from other $MoSe_2$ based solar cell [22], which is likely attributed to the large resistances of the device. The $MoSe_2$ monolayer being a direct gap helps electron hopping, as suggested in the literature [23], and therefore improves the efficiency of the solar cell. In terms of the (J–V) characteristic of $MoSe_2$ solar cells, shunt current effect is observed.

The parameters of the cells deduced from the characteristic (J–V) plot are summarized in the Table II.

TABLE II

Photovoltaic parameters of $ZnO/ZnS/MoSe_2$.

Solar cell configuration	$ZnO/ZnS/MoSe_2$
V_{oc} [V]	0.795
J_{sc} [mA/cm^2]	22.19
η [%]	17.51
V_{MPP} [V]	0.8
J_{MPP} [mA/cm^2]	21.89

Figure 4 shows the quantum efficiency (QE) of ($ZnO/ZnS/MoSe_2$) structure. A lower number of photons at the absorber layer would decrease the QE of the solar cells.

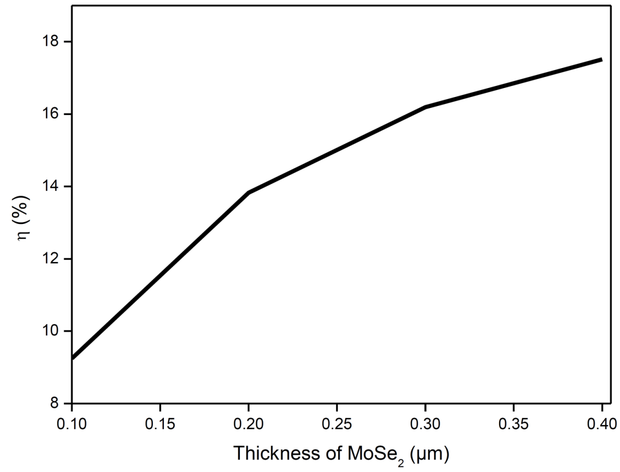

Fig. 2. Thickness of $MoSe_2$ layer effect on the efficiency.

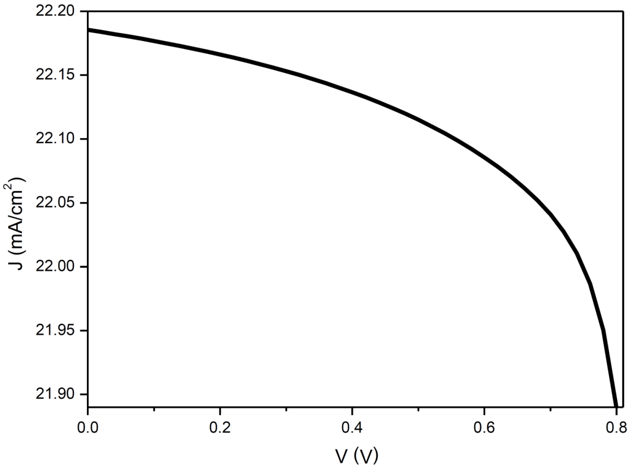

Fig. 3. J–V characteristics of $MoSe_2$ solar cells.

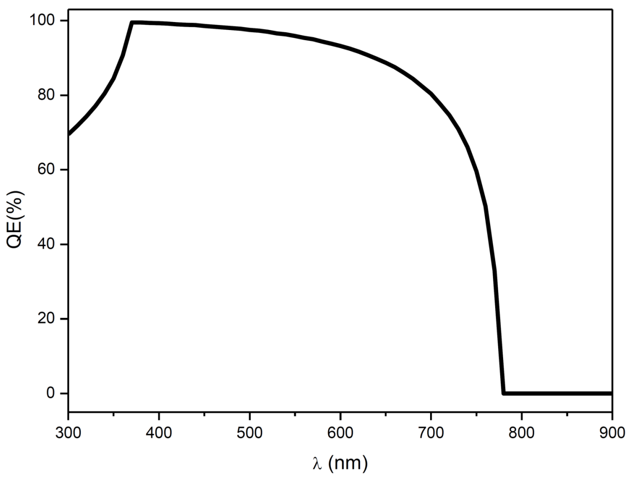

Fig. 4. Spectral response of $MoSe_2$ structure solar cell.

The QE of the $MoSe_2$ based solar cells similarly varies between 0 and 99.55%. The maximum value is obtained at 370 nm wavelength. The efficiency is 69.5% at the radiation of 300 nm and increases gradually with the increase in the wavelength to reach a maximum at 370 nm to 99.55%. Moreover, the Spectral response range of the $MoSe_2$ based solar cells covers the visible and near infrared spectral regions of 350 to 800 nm, which is favourable for the improvement of solar cell performance [24, 25].

4. Conclusion

The $ZnO/ZnS/MoSe_2$ based solar cell is analyzed using SCAPS-1D. Absorber layer thickness and defect density influences the performance of the solar cell. After optimizing all the parameters, the thickness of $MoSe_2$ films is selected as 0.4 μm for the best solar cell performance. The power conversion efficiency obtained is 17.51% and a current density (J_{sc}) of 22.19 mA/cm^2 is attained at the corresponding open circuit voltage (V_{oc}) of 0.8 V.

Acknowledgments

The authors thank to Marc Burgelman and his team at the University of Gent for the access of SCAPS-1D.

References

[1] S. Zaynabidinov, R. Aliev, M. Muydinova, B. Urmanov, *Appl. Solar Energy* **54**, 395 (2018).

[2] B. Zaidi, I. Saouane, C. Shekhar, *Silicon* **10**, 975 (2018).

[3] O. Martíneza, J. Mass, A. Tejero, B. Moralejo, V. Hortelano, M.A. González, J. Jiménez, V. Parra, *Acta Phys. Pol. A* **125**, 1013 (2014).

[4] A.O. Pudov, A. Kanevce, H. Al-Thani, J.R. Sites, F.S. Hasoon, *J. Appl. Phys.* **97**, 1063 (2005).

[5] B. Zaidi, B. Hadjoudja, B. Chouial et al., *Silicon* **10**, 975 (2018).

[6] L.Z. Hao, W. Gao, Y.J. Liu et al., *Nanoscale* **7**, 8304 (2015).

[7] C. Yang, Y. Yin, Y. Guo, *J. Phys. Chem. Lett.* **6**, 256 (2015).

[8] W. Kautek, H. Gerischer, *Electrochim. Acta* **26**, 1771 (1981).

[9] G. Wang, E. Palleau, T. Amand, S. Tongay et al., *Appl. Phys. Lett.* **106**, 112101 (2015).

[10] J. Verschraegen, M. Burgelman, *Thin Solid Films* **515**, 6276 (2007).

[11] K. Decock, S. Khelifi, M. Burgelman, *Thin Solid Films* **519**, 7481 (2011).

[12] M. Burgelman, P. Nollet, S. Degrave, *Thin Solid Films* **361**, 527 (2000).

[13] M. Burgelman, J. Verschraegen, S. Degrave et al., *Res. Appl.* **12**, 143 (2004).

[14] Y. Yuan, Z. Li, S. Wu et al., *Chem. Eng. J.* **350**, 335 (2018).

[15] X. Yuan, B. Zhou, X. Zhang et al., *Electrochim. Acta* **283**, 1163 (2018).

[16] H. Qi, W. Mi, H. Zhao, et al., *Mater. Lett.* **201**, 161 (2017).

[17] J. Wan, B. An, Z. Chen, et al., *J. Alloys Compd.* **750**, 499 (2018).

[18] S. Tongay, J. Zhou, C. Ataca, et al., *Nano Lett.* **12**, 5576 (2012).

[19] J. Ye, J. Li, J. Zhao, et al., *Nanoscale Res. Lett.* **10**, 454 (2015).

[20] Y. Shi, C. Hua, B. Li, et al. *Adv. Funct. Mater.* **23**, 1832 (2013).

[21] J. Tao, J. Chai, X. Lu, *Nanoscale* **7**, 2497 (2015).

[22] M. Shanmugam, T. Bansal, C.A. Durcan, B. Yu, *Appl. Phys. Lett.* **100**, 153901 (2012).

[23] M. Shanmugam, C.A.Durcan, B. Yu, *Nanoscale* **4**, 7399 (2012).

[24] Y. Liu,Y.X. Yu, W.D. Zhang, *J. Phys. Chem. C* **117**, 12949 (2013).

[25] W. Gu, F. Yang, C. Wu, Y. Zhang, M. Shi, X. Ma, *Nanoscale Res. Lett.* **9**, 662 (2014).